

Anomalous scaling behavior of the dynamical spin susceptibility of $\text{Ce}_{0.925}\text{La}_{0.075}\text{Ru}_2\text{Si}_2$

W. Knafo¹, S. Raymond¹, J. Flouquet¹, B. Fåk¹, M.A. Adams², P. Haen³, F. Lapierre³, S. Yates³, and P. Lejay³

¹ CEA-Grenoble, DSM/DRFMC/SPSMS, 38054 Grenoble Cedex 9, France

² ISIS Facility, Rutherford Appleton Laboratory, Chilton, Didcot, Oxon OX11 0QX, UK

³ CRTBT, CNRS, B.P. 166, 38042 Grenoble Cedex 9, France

(Dated: February 8, 2020)

Inelastic neutron scattering measurements have been performed on single crystals of $\text{Ce}_{0.925}\text{La}_{0.075}\text{Ru}_2\text{Si}_2$ in broad energy [0.1, 9.5 meV] and temperature [40 mK, 294 K] ranges in order to address the question of scaling behavior of the dynamical spin susceptibility at the quantum critical point of an itinerant magnetic system. For two wavevectors \mathbf{Q} corresponding to single site and antiferromagnetic spin fluctuations, it is found that the dynamical spin susceptibility $\chi''(\mathbf{Q}, E, T)$ is independent of temperature below a cut-off temperature $T_{\mathbf{Q}}$. Above $T_{\mathbf{Q}}$ a \mathbf{Q} -dependent scaling behavior of the form $T\chi''(\mathbf{Q}, E, T) = f_{\mathbf{Q}}[E/(a_{\mathbf{Q}}T^{\beta_{\mathbf{Q}}})]$ with $\beta_{\mathbf{Q}} < 1$ is obtained.

PACS numbers: 71.27.+a, 75.40.Gb, 78.70.Nx, 89.75.Da

1. INTRODUCTION

In many heavy fermions systems (HFS) a quantum phase transition (QPT) separates a non-magnetic from a magnetic ground state at $T = 0$ K. Such a transition is governed by the competition between Kondo screening of localized moments and RKKY-like intersite interactions. It can be tuned by applying an external pressure, a magnetic field or by chemical substitution. In the vicinity of a QPT, the critical fluctuations have a quantum feature characterized by an effective dimension $d^* = d + z$, d being the spatial dimension and z the dynamical exponent^{1,2,3,4}. The extra dimension z is relative to the imaginary time direction ($z = 2$ for antiferromagnetic fluctuations). When T is increased, a cross-over regime (also called quantum classical (QC)) sets up when the fluctuations lose their quantum features and become controlled by T . The dimension is then reduced from d^* to d . In a simple picture this can be seen as a finite-size scaling⁵, where the "finite size" $\tau_T \sim 1/T$ of the system in the time dimension is decreased when T is increased⁶: the time dimension is then progressively suppressed. If τ is the relaxation time of quantum fluctuations, the quantum regime is the low T regime for which $\tau_T > \tau$, when the dynamical properties behave as functions of $\omega\tau$ and do not depend on T . The cross-over regime is then expected for $\tau_T < \tau$, its dynamical properties behaving as functions of ω/T . Inelastic neutron scattering (INS) is a unique tool for studying dynamic magnetic properties. Enhancements of spin fluctuations (SF) have already been reported by INS around the QPT of HFS (see for example^{7,8,9}). The T -dependence of those low-energy excitations is believed to be related to the low-temperature non Fermi liquid behavior observed by bulk measurements near the quantum critical point (QCP) of such systems¹⁰. That is why it is necessary for the understanding of QPT to study precisely how SF evolve with T and to search for scaling laws specific to the QC regime. Several INS studies report ω/T scaling of the dynamical spin susceptibility in HFS or high T_C

superconductors^{11,12,13,14,15}. In particular, some insight was given by the detailed study of Schröder et al. at the QCP of $\text{CeCu}_{6-x}\text{Au}_x$ ¹¹: they obtained a collapse of the dynamical spin susceptibility on a single curve when plotted as $T^{0.75}\chi''(\omega, T) = f(\omega/T)$. A general form of this law was found to work with the same T -exponents for each vector of the reciprocal lattice and down to the smallest accessible temperatures. This \mathbf{Q} -dependence became the starting point of a local description of quantum criticality^{16,17}. Such a description is opposed to itinerant scenarii where the QPT is only driven by fluctuations at some critical wavevectors^{1,2,18,19}.

We have chosen here to search for a scaling behavior at the QCP of $\text{Ce}_{1-x}\text{La}_x\text{Ru}_2\text{Si}_2$, a HFS that has been extensively studied for about 20 years^{20,21,22,23,24}. This 3D Ising system has a QCP at $x_c \simeq 7.5\%$ that separates a paramagnetic ground state for $x < x_c$ from an antiferromagnetic ground state with the incommensurate propagation vector $\mathbf{k}_1 = (0.31 \ 0 \ 0)$ for $x > x_c$. Although the occurrence of small magnetic moments has been reported for $x \leq x_c$ ($0.02 \ \mu_B$ at $\mathbf{k}_1 = (0.31 \ 0 \ 0)$ below 2 K for $x = x_c$ ⁷ and $0.001 \ \mu_B$ also below 2 K for $x = 0.25$), a long range magnetic order with diverging correlation length is only obtained for $x > x_c$. Large single crystals are available, which makes it possible to investigate precisely the reciprocal space via INS. In this system, the observed excitations spectra consist of uncorrelated single site SF and of short range magnetic correlations that lead to enhanced antiferromagnetic SF with the wavevector \mathbf{k}_1 . Previous neutron measurements have shown the continuous behavior of the SF through the QCP^{23,24} and several tests led to a rather good accordance between Moriya's itinerant theory and experimental data^{7,18,21,26}. $\text{Ce}_{1-x}\text{La}_x\text{Ru}_2\text{Si}_2$ constitutes consequently an opportunity to study quantum criticality in a case for which the itinerancy of the $4f$ electrons is established. For this purpose, we present here new measurements at the critical concentration x_c that were made not only to benefit from much better statistics but also to measure a broader range of temperatures (between 40 mK and 294 K) and

energies (between 0.1 and 9.5 meV). Such extended data are required for a precise determination of the temperature dependence of the SF. In this paper we report an anomalous scaling behavior of the dynamical spin susceptibility at the QCP of $\text{Ce}_{1-x}\text{La}_x\text{Ru}_2\text{Si}_2$: instead of ω/T , ω/T^{β_Q} scalings with $\beta_Q < 1$ are obtained. Contrary to the other cases reported in literature, the laws found here depend on the wavevector and each one is characterized by a different low-temperature cut-off below which a nearly T -independent quantum regime is obtained.

2. EXPERIMENTAL DETAILS

The single crystals of $\text{Ce}_{0.925}\text{La}_{0.075}\text{Ru}_2\text{Si}_2$ studied here have been grown by the Czochralsky method. They crystallize in the body centered tetragonal $I4/mmm$ space group with the lattice parameters $a = b = 4.197 \text{ \AA}$ and $c = 9.797 \text{ \AA}$. A single crystal of 250 mm^3 was used for the INS measurements and a smaller one of 3 mm^3 for the DC susceptibility measurements. INS measurements were carried out on the cold and thermal triple-axis spectrometers IN12 and IN22 at the ILL (Grenoble, France). The (001) plane was investigated. 60'-open-open and open-open-open set-up were used on IN12 and IN22, respectively. A beryllium filter on IN12 and a pyrolytic graphite (PG) filter on IN22 were added to eliminate higher-order contaminations. In both cases PG was used for the vertically focusing monochromator and for the horizontally focusing analyzer. The final neutron energy was fixed to 4.65 meV on IN12 and to 14.7 meV on IN22 with the resulting energy resolutions of about 0.17 meV on IN12 and 1 meV on IN22 (FWHM of the incoherent signal). For temperatures between 2.5 and 80 K the high-energy points obtained on IN22 were combined with the ones obtained on IN12, with an appropriate scale factor chosen for the collapse of the data in their common range 1.9-2.5 meV. A complementary neutron experiment was carried out on the inverted-geometry time-of-flight spectrometer IRIS at ISIS (Didcot, U.K.) using a fixed final neutron energy of 1.84 meV (PG analyzer) resulting in 18 μeV resolution FWHM. The susceptibility measurements were performed both in a commercial SQUID DC magnetometer for temperatures between 5 and 300 K and in a dilution refrigerator SQUID DC magnetometer for temperatures between 250 mK and 5 K, with the magnetic field along the [001] easy axis in both cases.

3. TEMPERATURE DEPENDENCE OF SPIN FLUCTUATIONS

The data presented here consist in energy scans obtained by INS at two wavevectors: the antiferromagnetic momentum transfer $\mathbf{Q}_1 = (0.69 \ 1 \ 0) = \boldsymbol{\tau} - \mathbf{k}_1$, where $\boldsymbol{\tau} = (1 \ 1 \ 0)$ is a reciprocal lattice vector, and the single site wavevector $\mathbf{Q}_{SS} = (0.44 \ 1 \ 0)$, where no spatial correlations are observed. In FIG. 1 the excitations spec-

tra obtained at those two vectors are plotted for three representative temperatures: their shape is characteristic of a relaxation process. At $T = 5 \text{ K}$, antiferromagnetic fluctuations are enhanced in comparison with the single site ones. When the temperature is raised the difference between the two signals is attenuated and above the correlation temperature $T_{corr} \simeq 80 \text{ K}$ they are almost identical; the system has lost its antiferromagnetic correlations. The observed intensity is proportional to the scattering function $S(\mathbf{Q}, E, T)$ (where $E = \hbar\omega$), from which the imaginary part of the dynamical susceptibility $\chi''(\mathbf{Q}, E, T)$ is deduced using:

$$S(\mathbf{Q}, E, T) = \frac{1}{\pi} \frac{1}{1 - e^{-E/k_B T}} \chi''(\mathbf{Q}, E, T). \quad (1)$$

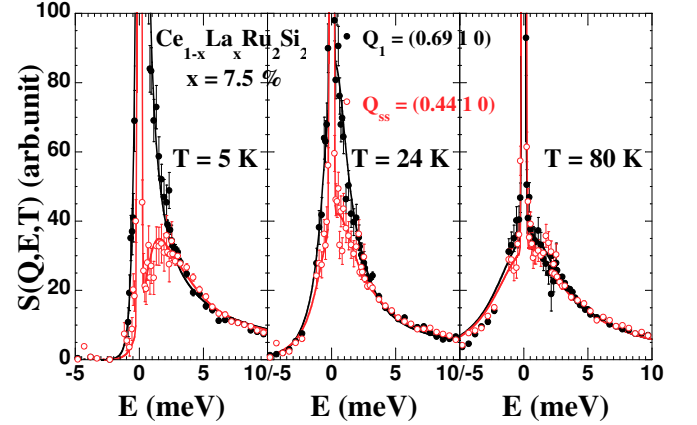


FIG. 1: INS spectra obtained at $T = 5, 24$ and 80 K for the momentum transfers \mathbf{Q}_1 and \mathbf{Q}_{SS} . A constant background deduced from the scattering at low temperature and negative energy transfers has been subtracted. The signal at $E = 0$ corresponds to the incoherent elastic background. The lines are the fits to the data.

For the two wavevectors the dynamical susceptibility is well fitted by a single quasi elastic Lorentzian shape of the form:

$$\chi''(\mathbf{Q}, E, T) = \frac{A(\mathbf{Q}, T)}{\Gamma(\mathbf{Q}, T)} \frac{E/\Gamma(\mathbf{Q}, T)}{1 + (E/\Gamma(\mathbf{Q}, T))^2} \quad (2)$$

that corresponds to the simplest approximation that can be made to treat the spin fluctuations. The general form of the dynamical susceptibility is the Fourier transform of a single exponential decay of relaxation rate $\Gamma(\mathbf{Q}, T)$. It can be expressed by:

$$\begin{aligned} \chi(\mathbf{Q}, E, T) &= \chi'(\mathbf{Q}, E, T) + i\chi''(\mathbf{Q}, E, T) \\ &= \frac{A(\mathbf{Q}, T)}{\Gamma(\mathbf{Q}, T) - iE}. \end{aligned} \quad (3)$$

In such a case, the static susceptibility is given by the Kramers-Kronig relation:

$$\begin{aligned} \chi'(\mathbf{Q}, T) &= \chi'(\mathbf{Q}, E = 0, T) = \frac{1}{\pi} \int_{-\infty}^{\infty} \frac{\chi''(\mathbf{Q}, E, T)}{E} dE \\ &= \frac{A(\mathbf{Q}, T)}{\Gamma(\mathbf{Q}, T)} \end{aligned} \quad (4)$$

However, in a previous thermal INS experiment on CeRu_2Si_2 , Adroja et al. observed a broad crystal field (CF) excitation at about 30 meV that dominates the excitation spectra for $E > 10$ meV, its width (HWHM) being about 15 meV²⁷. Bulk susceptibility measurements also indicate that the CF scheme do not change very much with concentration x in $\text{Ce}_{1-x}\text{La}_x\text{Ru}_2\text{Si}_2$ ²⁰. It is thus reasonable to consider that in $\text{Ce}_{0.925}\text{La}_{0.075}\text{Ru}_2\text{Si}_2$, as well as in CeRu_2Si_2 , the CF excitations dominate the low-energy SF for $E > 10$ meV. Instead of (4) it is finally better to approximate the static susceptibility of the low-energy SF by introducing an energy cut-off of 10 meV such as:

$$\chi'(\mathbf{Q}, T) = \frac{2}{\pi} \int_0^{10} \frac{\chi''(\mathbf{Q}, E, T)}{E} dE \quad (5)$$

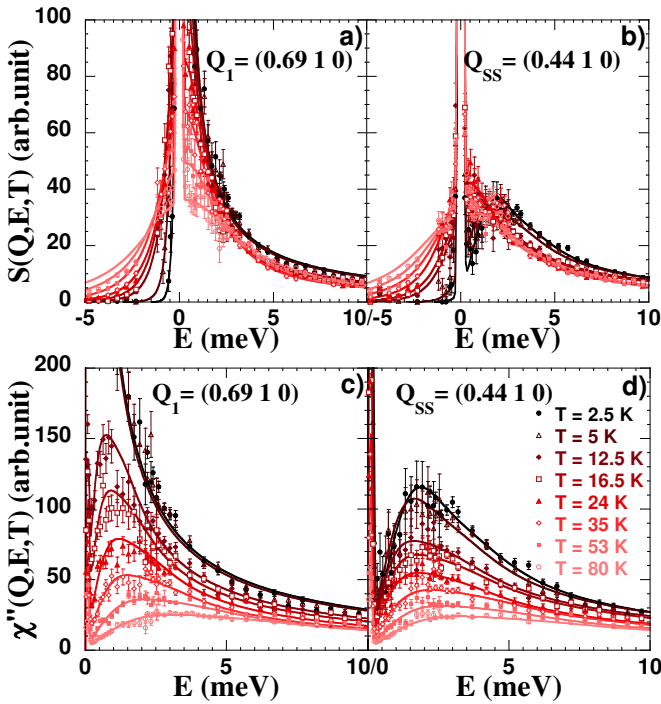


FIG. 2: Scattering function $S(\mathbf{Q}, E, T)$ a) at \mathbf{Q}_1 b) at \mathbf{Q}_{ss} and dynamical susceptibility $\chi''(\mathbf{Q}, E, T)$ c) at \mathbf{Q}_1 d) at \mathbf{Q}_{ss} for $2.5 < T < 80$ K. The lines are the fits to the data.

$S(\mathbf{Q}, E, T)$ and its fits using (2) are plotted for the two wavevectors and $2.5 < T < 80$ K in FIG. 2 a and b. $S(\mathbf{Q}_1, E, T)$, which corresponds to antiferromagnetic SF, is shown in FIG. 2 a: it is found to decrease in intensity and to broaden when T is increased. For single site SF, the scattering intensity $S(\mathbf{Q}_{ss}, E, T)$, which is plotted in FIG. 2 b, is characterized by the collapse of the data on a single curve for positive energy transfers and $T > 5$ K. The negative energy points are strongly T -dependent because of the detailed balance condition $S(\mathbf{Q}, -E, T) = \exp(-E/k_B T) S(\mathbf{Q}, E, T)$. Such a behavior was also reported for the polycrystalline compounds UCu_4Pd and $\text{CeRh}_{0.8}\text{Pd}_{2.2}\text{Sb}$, where the scattering is temperature independent for positive energy transfers^{12,13}.

For $T = 2.5$ and 5 K the single site signal $S(\mathbf{Q}_{ss}, E, T)$ moves to higher energies. Although better fits are obtained using an inelastic symmetrized Lorentzian instead of the quasielastic Lorentzian shape (2), it is difficult to conclude about their inelasticity, since the widths of these peaks are too important. For both \mathbf{Q}_1 and \mathbf{Q}_{ss} , a strong T -dependence of the dynamical susceptibility $\chi''(\mathbf{Q}, E, T)$ deduced from (1) (and its fits using (2)) is shown in FIG. 2 c and d. Contrary to $S(\mathbf{Q}, E, T)$, $\chi''(\mathbf{Q}, E, T)$ has a decreasing intensity for both wavevectors and is strongly broadened when T is raised. Finally, for each spectrum, the relaxation rate $\Gamma(\mathbf{Q}, T)$ and the static susceptibility $\chi'(\mathbf{Q}, T)$ are extracted using (2) and (5). In the next two subsections, the results of the fits of low-energy SF are separately analyzed for the antiferromagnetic and single site momentum transfers \mathbf{Q}_1 and \mathbf{Q}_{ss} .

3.1. Antiferromagnetic spin fluctuations

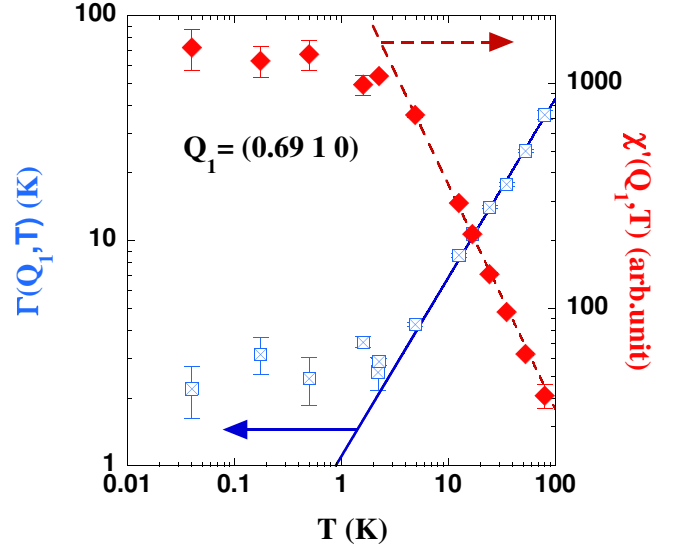


FIG. 3: Variations with T of $\Gamma(\mathbf{Q}_1, T)$ and $\chi'(\mathbf{Q}_1, T)$. The full and dashed lines correspond to the high-temperature fits of the relaxation rate $\Gamma(\mathbf{Q}_1, T) = 1.1T^{0.8}$ and of the static susceptibility $\chi'(\mathbf{Q}_1, T) = 3550/T$, respectively.

The analysis of the antiferromagnetic SF at the momentum transfer \mathbf{Q}_1 is only made below $T_{corr} \simeq 80$ K, higher temperatures at this wavevector corresponding then to single site SF. The variations with T of the relaxation rate $\Gamma(\mathbf{Q}_1, T)$ and the static susceptibility $\chi'(\mathbf{Q}_1, T)$ for antiferromagnetic SF are plotted in FIG. 3. As seen, there are clearly two different regimes: a nearly T -independent low-temperature and a strongly T -dependent high-temperature regimes.

Below a characteristic temperature of $T_1 \simeq 3$ K, $\chi''(\mathbf{Q}_1, E, T)$ does not depend on T . Moreover, the relaxation rate is found to have the value $\Gamma(\mathbf{Q}_1, T) \simeq k_B T_1$

in this regime: this is thus the low-temperature regime for which $\tau < \tau_T$, with $\tau = 1/\Gamma(\mathbf{Q}_1, T = 0) \sim 1/T_1$ and $\tau_T \sim 1/T$, as presented using a simple picture of scaling in the introduction. The saturation of antiferromagnetic SF corresponds thus to their quantum regime. Because of the limited resolution on IN12 and IN22, a complementary experiment was made on the time-of-flight backscattering spectrometer IRIS. Measurements were carried out at 100 mK and 2 K with a resolution of 18 μeV . $\chi''(\mathbf{Q}, E, T)$ was found not to depend on T for $\mathbf{Q} \simeq \mathbf{Q}_1$, which confirms the saturation of antiferromagnetic SF at temperatures below T_1 .

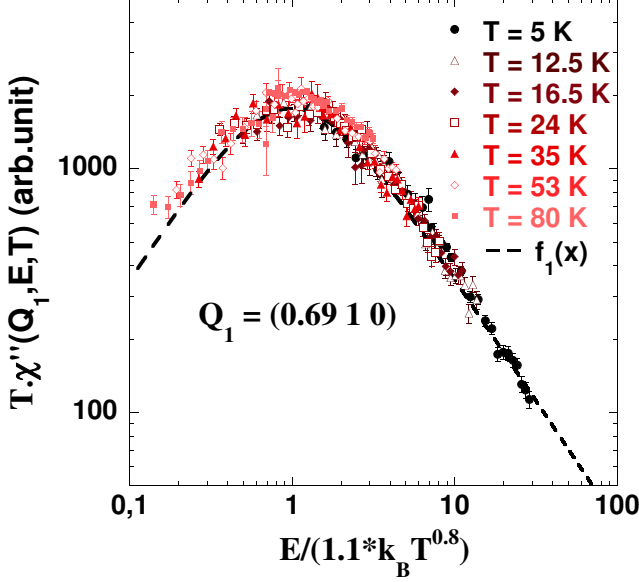


FIG. 4: Scaling behavior of the low-energy SF obtained for $3 < T < 80$ K at \mathbf{Q}_1 . The dynamical susceptibility follows the scaling law $T\chi''(\mathbf{Q}_1, E, T) = f_1[E/(a_1 T^{0.8})]$ with $f_1(x) = C_1 * x/(1 + x^2)$

At higher temperatures, $T_1 < T < T_{corr}$, the antiferromagnetic SF become controlled by T such that T -power laws can be extracted for $\chi'(\mathbf{Q}_1, T)$ and $\Gamma(\mathbf{Q}_1, T)$:

$$\chi'(\mathbf{Q}_1, T) = C_1/T^{\alpha_1} \quad \text{and} \quad \Gamma(\mathbf{Q}_1, T) = a_1 T^{\beta_1} \quad (6)$$

with

$$\begin{aligned} \alpha_1 &= 1 \pm 0.05, & C_1 &= 3550 \pm 100 \text{ arb. unit}, \\ \beta_1 &= 0.8 \pm 0.05, & \text{and} \quad a_1 &= 1.1 \pm 0.05 \text{ SI unit}. \end{aligned}$$

To be more precise, the characteristic temperature T_1 has been defined by the intercept of the two asymptotic regimes obtained at low and high temperatures, the same intercept being given for $\chi'(\mathbf{Q}_1, T)$ and $\Gamma(\mathbf{Q}_1, T)$. Finally, the neutron data can be plotted as $T\chi''(\mathbf{Q}_1, E, T) = f_1[E/(a_1 T^{0.8})]$ such that all the points measured for $T_1 < T < T_{corr}$ at the antiferromagnetic wavevector collapse on the single Lorentzian curve $f_1(x) = C_1 x/(1 + x^2)$ with $x = E/(a_1 T^{0.8})$ (see FIG. 4). In the discussion, we will focus on the anomalous form of

this scaling law obtained for the antiferromagnetic low-energy SF.

3.2. Single site spin fluctuations

The variations with T of the relaxation rate $\Gamma(\mathbf{Q}_{SS}, T)$ and the static susceptibility $\chi'(\mathbf{Q}_{SS}, T)$ of single site SF are plotted in FIG. 5. As for the antiferromagnetic SF, we can define a characteristic temperature $T_{SS} \simeq 17$ K at the intercept of the asymptotic low and high-temperature regimes. Below T_{SS} , $\chi''(\mathbf{Q}_{SS}, E, T)$ does not depend on T , and $\Gamma(\mathbf{Q}_{SS}, T) \simeq k_B T_{SS}$. For T larger than T_{SS} , T -power laws can be extracted; the fits made on $\chi'(\mathbf{Q}_{SS}, T)$ for $T \geq 80$ K and on $\Gamma(\mathbf{Q}_{SS}, T)$ for $T \geq 20$ K give:

$$\chi'(\mathbf{Q}_{SS}, T) = C_{SS}/T^{\alpha_{SS}} \quad \text{and} \quad \Gamma(\mathbf{Q}_{SS}, T) = a_{SS} T^{\beta_{SS}} \quad (7)$$

with

$$\begin{aligned} \alpha_{SS} &= 1 \pm 0.1, & C_{SS} &= 2740 \pm 200 \text{ arb. unit}, \\ \beta_{SS} &= 0.6 \pm 0.2, & \text{and} \quad a_{SS} &= 3.1 \pm 0.5 \text{ SI unit}. \end{aligned}$$

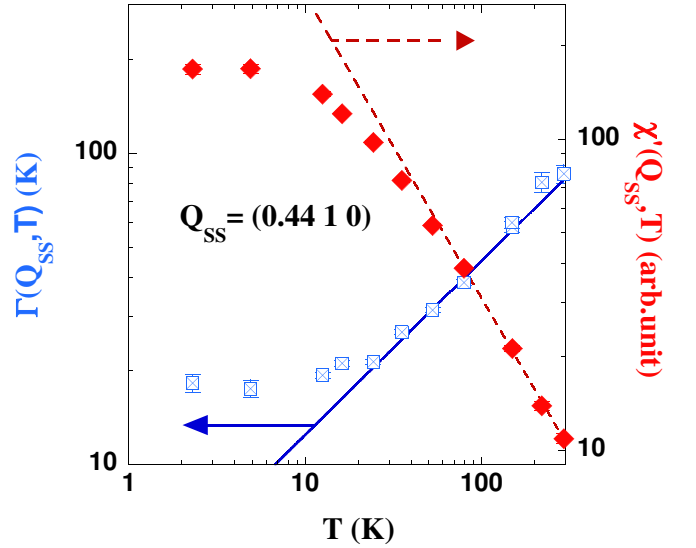


FIG. 5: Variations with T of $\Gamma(\mathbf{Q}_{SS}, T)$ and $\chi'(\mathbf{Q}_{SS}, T)$. The full and dashed lines correspond to the high temperatures fits of the relaxation rate $\Gamma(\mathbf{Q}_{SS}, T) = 3.1 T^{0.6}$ and of the static susceptibility $\chi'(\mathbf{Q}_{SS}, T) = 2740/T$, respectively.

However, higher energy scales and smaller intensities make the study of single site SF more difficult than for the antiferromagnetic case. Indeed, the single site quantum regime differs from the antiferromagnetic one in its energy scale $k_B T_{SS}$ that is 5 times larger than the antiferromagnetic energy scale $k_B T_1$. This results in an overlap with the higher energy CF excitation that makes the uncertainties on α_{SS} and β_{SS} larger than in the antiferromagnetic case. As a consequence, at high temperatures the exponent β_{SS} is somewhat overestimated. This

value of $\beta_{SS} = 0.6 \pm 0.2$ should be related to the value of 0.5 predicted and observed for Kondo systems at high temperatures^{28,29,30,31}. The estimation of α_{SS} seems correct because the corresponding Curie-like behavior of $\chi'(\mathbf{Q}_{SS}, T)$ is in good agreement with bulk susceptibility (see discussion). Since the energy scale $k_B T_{SS}$ is large, the analysis of the T -dependent regime must be made at high temperatures: for T higher than 100 K the thermal population of the first excited CF state becomes non negligible and fluctuations on this level contribute also to low-energy SF. In the present analysis we suppose that the first excited state behaves similarly to the ground state when both are populated at high temperatures. Finally, we believe that, without the crystal field contribution, the single site low-energy dynamical susceptibility should scale as $T\chi''(\mathbf{Q}_{SS}, E, T) = f_{SS}[E/(a_{SS}T^{0.5})]$ for $T > T_{SS}$, with $f_{SS}(x) = C_{SS}x/(1+x^2)$.

4. DISCUSSION

4.1. Comparison with bulk susceptibility

The bulk susceptibility χ_{bulk} , measured along the c axis, is compared with the microscopic static susceptibilities $\chi'(\mathbf{Q}_1, T)$ and $\chi'(\mathbf{Q}_{SS}, T)$ in FIG. 6. For $T > 100$ K, $\chi_{bulk}(T)$ follows a Curie-Weiss law with a Curie temperature $\theta \simeq 20$ K, such as $\chi_{bulk}(T) = C/(T - \theta)$. For $T > 100$ K, the static susceptibilities $\chi'(\mathbf{Q}, T)$ deduced from INS have also been fitted by Curie-like laws that are undistinguishable from Curie-Weiss laws, within the uncertainty in $\chi'(\mathbf{Q}, T)$. From the CF scheme of $\text{Ce}_{1-x}\text{La}_x\text{Ru}_2\text{Si}_2$ ^{32,33}, it is known that the Van Vleck term is negligible in the bulk c -axis susceptibility³⁴. Since the high-energy CF excitation is not taken into account in the integrated susceptibilities from INS, both macroscopic and microscopic susceptibilities $\chi_{bulk}(T)$ and $\chi'(\mathbf{Q}, T)$ correspond only to low-energy SF. The bulk susceptibility being a measure at the wavevector $\mathbf{Q} = 0$, we have $\chi_{bulk}(T) = \chi'(\mathbf{Q} = 0, T)$ when $\chi'(\mathbf{Q}, T)$ is obtained using (5). For $T > T_{corr}$, there are no more magnetic correlations and we can adjust the different data on a single scale. $\chi_{bulk}(T)$ can also be treated similarly to $\chi'(\mathbf{Q}_1, T)$ and $\chi'(\mathbf{Q}_{SS}, T)$. As for the neutron data, we can define a characteristic temperature $T^* \simeq 16$ K at the intercept of the asymptotic low-temperature and high-temperature regimes. In the quantum regime, the hierarchy $\chi'(\mathbf{Q}_{SS}, 0) < \chi_{bulk}(0) < \chi'(\mathbf{Q}_1, 0)$ is due to that the low-energy ferromagnetic SF are more important at low temperatures than the single site ones, both being much smaller than the antiferromagnetic SF. This small enhancement of ferromagnetic SF is linked to the metamagnetic transition in the system $\text{Ce}_{1-x}\text{La}_x\text{Ru}_2\text{Si}_2$: the application of a magnetic field induces an enhancement of ferromagnetic SF that is maximum at the metamagnetic field H_m ^{20,35,36,37,38}. We can also express $\chi'(\mathbf{Q}_1, T)$

and $\chi'(\mathbf{Q}_{SS}, T)$ in CGS units, which gives:

$$\begin{aligned} T_1 \cdot \chi'(\mathbf{Q}_1, 0) &= 1.00 \pm 0.1 \text{ K.emu.mol}^{-1}\text{Oe}^{-1}, \\ T_{SS} \cdot \chi'(\mathbf{Q}_{SS}, 0) &= 0.97 \pm 0.1 \text{ K.emu.mol}^{-1}\text{Oe}^{-1}, \\ \text{and } T^* \cdot \chi_{bulk}(0) &= 1.09 \pm 0.1 \text{ K.emu.mol}^{-1}\text{Oe}^{-1}. \end{aligned}$$

If T_Q is the characteristic temperature of the SF at the wavevector \mathbf{Q} , we have thus $T_Q \cdot \chi'(\mathbf{Q}, 0)$ independent of \mathbf{Q} , within the error bars. Since $\Gamma(\mathbf{Q}_1, 0) \simeq k_B T_1$ and $\Gamma(\mathbf{Q}_{SS}, 0) \simeq k_B T_{SS}$, we can assume $\Gamma(\mathbf{Q} = 0, 0) \simeq k_B T^*$, so that the product $\Gamma(\mathbf{Q}, 0) \cdot \chi'(\mathbf{Q}, 0)$ is independent of \mathbf{Q} . Hence, the low-temperature magnetic properties are in good agreement with a Fermi liquid description of a correlated system governed by an antiferromagnetic instability, for which $\Gamma(\mathbf{Q}, T) \cdot \chi'(\mathbf{Q}, T)$ is expected to be constant^{18,39,40}. This Fermi liquid picture is broken when, at high temperatures, $\Gamma(\mathbf{Q}, T) \cdot \chi'(\mathbf{Q}, T)$ drops because of the different T -behaviors of $\Gamma(\mathbf{Q}, T)$ and $1/\chi'(\mathbf{Q}, T)$.

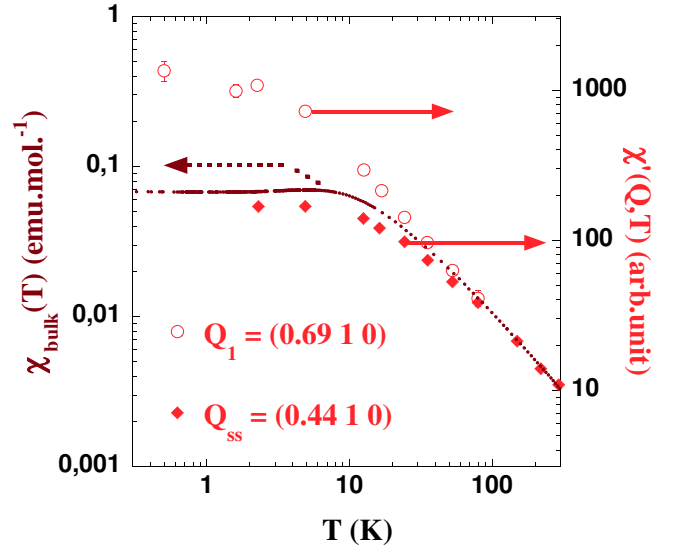


FIG. 6: Variations with T of $\chi'(\mathbf{Q}_1, T)$ and $\chi'(\mathbf{Q}_{SS}, T)$ in comparison with $\chi_{bulk}(T)$

For $T < 5$ K, the slight increase of $\chi_{bulk}(T)$ when T is raised (see FIG. 7) is believed to be linked to a Kondo lattice hybridization gap. Although INS single site data alone are not accurate enough to conclude about the opening of a gap below 5 K, we think that their probable inelastic shape (see section 3) is related to the gap observed in $\chi_{bulk}(T)$. We are also aware that the error in $\chi'(\mathbf{Q}_{SS}, T)$ is too important to see the slight variations with T of this quantity below 5 K, as observed for $\chi_{bulk}(T)$.

4.2. About theoretical scenari

Contrary to the simple picture of scaling presented in the introduction⁶ but also to the different cases of scaling

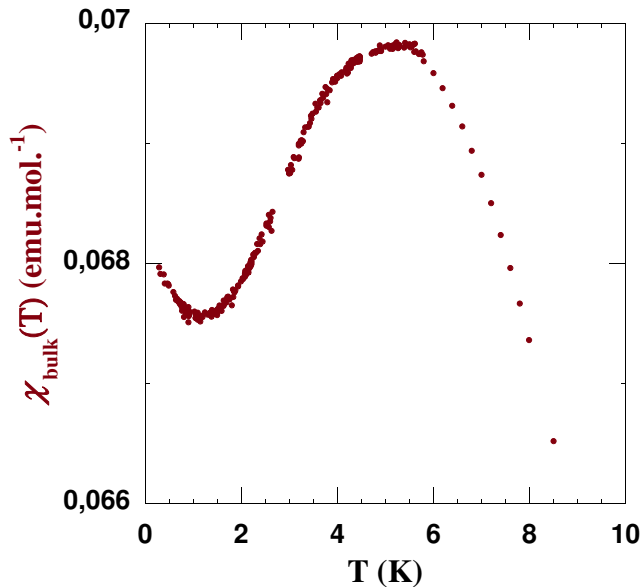


FIG. 7: Low temperatures variations of $\chi_{bulk}(T)$.

reported in the literature^{11,12,13,14,15}, we obtain ω/T^{β_Q} instead of ω/T scalings of the dynamical spin susceptibility of low-energy SF. Even if single site SF are not determined as precisely as antiferromagnetic SF, we have showed that low-energy SF of $\text{Ce}_{0.925}\text{La}_{0.075}\text{Ru}_2\text{Si}_2$ obey scaling laws that depend on the wavevector \mathbf{Q} , each one being characterized by a different low-temperature cut-off $T_{\mathbf{Q}}$ below which a T -independent Fermi liquid-like quantum regime is obtained. While a local description of quantum criticality was proposed to explain the behavior of $\text{CeCu}_{6-x}\text{Au}_x$ ^{11,16,17}, the itinerant character of our system is a key element to understand its behavior^{7,21,23,24}, and a scenario for which the QPT is driven by itinerant magnetism should be preferred. However, our system does not enter the framework of existing itinerant theories for QPT^{1,2,18,19}: two main discrepancies are obtained between theoretical and experimental features.

A first disagreement comes from the saturation below a finite temperature $T_1 \simeq 3$ K of $\chi''(\mathbf{Q}_1, E, T)$: we do not observe any divergence of the dynamical spin susceptibility at the QPT of $\text{Ce}_{1-x}\text{La}_x\text{Ru}_2\text{Si}_2$ and a low-temperature cut-off has to be taken into account. The saturation of antiferromagnetic SF at the QPT of this system was already reported for both cases of tuning by concentration or pressure^{23,24}. The origin of this cut-off is not yet well understood. It could be linked to the appearance of a tiny magnetic moment below $T_m = 2$ K $\simeq T_1$ ⁷. In such a case this small moment would not come from the disorder introduced by substitution and it would be intrinsically related to the finite value of T_1 . We must also consider that in the paramagnetic compound CeRu_2Si_2 , a very small moment is observed below the same characteristic temperature $T_m = 2$ K²⁵, while the low-temperature cut-off is then $T_1 \simeq 10$ K⁴¹. Small magnetic moments have also been reported for URu_2Si_2

and UPt_3 ⁴³.

The second discrepancy comes from that, in the QC regime, itinerant SF theories^{1,2,18,19} predict for 3D antiferromagnetic SF a ω/T^{β} scaling law with $\beta = 3/2$ instead of our experimental $\beta_1 = 0.8$; more generally, a value of β smaller than 1 can not be obtained in the theories of QPT based on universality^{3,4}. However, itinerant SF theories suppose that the Fermi surface is already fully formed, implying that the single site SF do not depend on T and thus that $T < T_{SS}$. Since antiferromagnetic SF saturate below $T_1 \simeq 3$ K, a search for $\beta = 3/2$ scaling could only be done in the range $T_1 < T < T_{SS}$. Not only the closeness of T_1 and T_{SS} but also the error done when estimating $\Gamma(\mathbf{Q}_1, T)$ make it very difficult to verify this. Contrary to the general framework of QPT theories, two kinds of scaling laws are obtained here: a critical antiferromagnetic and a non critical single site scalings, the two being undoubtedly linked. The critical antiferromagnetic SF, studied here at the wavevector \mathbf{Q}_1 , are believed to govern the QPT, in contrary to the non critical single site SF, studied at the wavevector \mathbf{Q}_{SS} . They correspond to RKKY-like and Kondo impurity physics, respectively, thus to different orders of interaction between conduction and f electrons: they consequently cannot be treated separately. A theory including the variations with T of single site SF is thus needed to explain the anomalous scaling law we obtain at the critical antiferromagnetic wavevector for $T > T_1$. For single site SF, an impurity Kondo model could be a good way to explain the Curie-like static susceptibility and the $T^{1/2}$ behavior of the relaxation rate for T sufficiently higher than T_{SS} , T_{SS} corresponding to the Kondo temperature of the system^{28,29,30,31,44}. Critical antiferromagnetic correlations should then be taken into account in an itinerant picture to explain the enhancement of antiferromagnetic SF at low temperatures and the temperature dependence of their relaxation rate and static susceptibility for $T_1 < T < T_{corr}$.

4.3. Comparison with other compounds.

In the present study, we have determined the energy and temperature dependence of the SF at the QCP of $\text{Ce}_{1-x}\text{La}_x\text{Ru}_2\text{Si}_2$. The use of single crystals on triple-axis spectrometers allowed us to obtain information on the SF at different wavevectors \mathbf{Q} . We found that the scaling behavior for the critical antiferromagnetic wavevector \mathbf{Q}_1 is different from the one obtained for the single site wavevector \mathbf{Q}_{SS} . In earlier work on the scaling properties of the SF near the QPT of other HFS, such as $\text{UCu}_{5-x}\text{Pd}_x$, $\text{Ce}(\text{Ru}_{1-x}\text{Fe}_x)_2\text{Ge}_2$, and $\text{CeRh}_{1-x}\text{Pd}_x\text{Sb}$ ^{12,13,14}, the use of polycrystalline samples on time-of-flight spectrometers made it more difficult to establish with precision any \mathbf{Q} -dependence of the SF.

In the case of the QCP of the HFS $\text{CeCu}_{6-x}\text{Au}_x$ (obtained for $x_c = 0.1$), Schröder et al. benefited from the use of a single crystal and from the combination of triple-

TABLE I: Comparison of characteristic physical quantities of CeCu₆ and CeRu₂Si₂^{21,23,24,41,42,46,47}

	CeCu ₆	CeRu ₂ Si ₂
γ^a	1.5 JK ⁻² mol ⁻¹	360 mJK ⁻² mol ⁻¹
T_γ^{*a}	0.2 K	3 K
T_ρ^{*b}	0.1 K	0.3 K
T_{SS}	5 K	23 K
T_1	2 K	10 K
T_{corr}	4 K	40 K
P_c^c	-4 kbar	-3 kbar

^a $C(T)/T = \gamma$ for $T < T_\gamma^*$

^b $\rho(T) = \rho(0) + AT^2$ for $T < T_\rho^*$

^cCorresponding pressures of the QCP of CeCu_{6-x}Au_x and Ce_{1-x}La_xRu₂Si₂

axis and time-of-flight techniques^{11,45}. The first study, using a triple-axis spectrometer, established a scaling law of the form $T^{0.75}\chi''(\omega, T) = f(\omega/T)$ at an antiferromagnetic wavevector⁴⁵. However, the extension of this law to other parts of the reciprocal lattice was done using a time-of-flight spectrometer¹¹, which limits the information that can be obtained concerning the \mathbf{Q} -dependence. Nevertheless, they found a single general form of scaling for every \mathbf{Q} of the reciprocal lattice. They also found their scaling law to work down to $T = 0$, as theoretically expected for critical SF at a QCP. In TABLE I are reported the main physical quantities that characterize the paramagnetic heavy fermion compounds CeCu₆ and CeRu₂Si₂ at low temperatures. For those two compounds, a Fermi liquid regime is obtained at low temperatures and characterizes their strong coupling renormalized state: the linear coefficient γ of the specific heat is found to be constant and highly renormalized for temperatures $T < T_\gamma^{*21}$, and the resistivity behaves as $\rho(0) + AT^2$ for $T < T_\rho^{*21,46}$. The temperatures T_1 , T_{SS} , and T_{corr} have been obtained by INS^{41,47}, as in the present study. As seen in TABLE I, the characteristic temperatures of CeCu₆ are about 5-10 times smaller than the corresponding ones of CeRu₂Si₂. Moreover, the QCP of CeCu_{6-x}Au_x and Ce_{1-x}La_xRu₂Si₂ are separated from their parent compounds CeCu₆ and CeRu₂Si₂ by the respective equivalent pressures of -4 kbar and -3 kbar^{23,24,42}. Because of these similar pressures, we believe that for CeCu_{5.9}Au_{0.1}, the characteristic temperatures are finally also about 5-10 times smaller than those of Ce_{0.925}La_{0.075}Ru₂Si₂. As well as the cut-off temperature $T_1 \simeq 3$ K is found to characterize the critical SF at the QCP of Ce_{1-x}La_xRu₂Si₂, the QCP of CeCu_{6-x}Au_x could thus have a cut-off temperature for its critical SF of order 0.3-0.6 K. Because of smaller characteristic temperatures and energies, in CeCu_{5.9}Au_{0.1} the quantum regime of the critical SF is thus much more difficult to distinguish from the classical scaling regime, and no saturation

of SF at low temperatures has been yet established by INS.

Finally, our results are quite similar to those of a recent work made by Bao et al.¹⁵. They measured by INS the antiferromagnetic fluctuations of a single crystal of La₂Cu_{0.94}Li_{0.06}O₄, using a triple-axis spectrometer. Contrary to the former systems, this system is not a HFS and is located in the Fermi liquid ground state region in the vicinity of a QCP. However, as in the present work, Bao et al. obtained a low-temperature quantum regime for which the dynamical susceptibility is found not to depend on T , and a high-temperature regime for which a scaling behavior is obtained, the relaxation rate $\Gamma(T)$ being in this case proportional to T and the static susceptibility $\chi(T)$, deduced from INS, following a Curie law.

5. CONCLUSION

A detailed study of the T -dependance of SF in Ce_{0.925}La_{0.075}Ru₂Si₂ has been carried out in this work. For each of the two antiferromagnetic and single site wavevectors \mathbf{Q}_1 and \mathbf{Q}_{SS} , a cut-off temperature T_Q delimits a low temperatures T -independent Fermi liquid-like quantum regime from a high-temperature scaling regime governed by T . The cut-off temperatures $T_1 \simeq 3$ K and $T_{SS} \simeq 17$ K are obtained for antiferromagnetic and single site SF, respectively. Several discrepancies with itinerant theories of QCP have been established: i) at low temperatures, while antiferromagnetic SF are enhanced in comparison with the single site ones, they saturate below T_1 and thus do not diverge when T tends to zero. ii) For each wavevector, high-temperature T -power laws can be extracted for the static susceptibility and the relaxation rate, so that the dynamical spin susceptibility is found to follow anomalous scaling of the form $T\chi''(\mathbf{Q}, E, T) = f_Q[E/(aQT^{\beta_Q})]$ above T_Q . Anomalous exponent $\beta_Q < 1$ is observed, which is incompatible with QPT theories. This is probably because these scaling laws are obtained in a T -range where single site SF are temperature dependent. Even at the QCP of an itinerant heavy fermion system, a Kondo impurity non critical scaling should thus be taken into account to understand the antiferromagnetic critical scaling which governs the QPT.

Acknowledgments

We thank D.T. Adroja and B.D. Rainford for sending us unpublished results on CF measurements in CeRu₂Si₂, and M.A. Continentino, M. Lavagna, C. Pépin, B. Coqblin, C. Lacroix, S. Burdin, Y. Sidis, A. Murani, N. Bernhoeft, and L.P. Regnault for very useful discussions.

- ¹ J.A. Hertz, Phys. Rev. B **14**, 1165 (1976).
- ² A.J. Millis, Phys. Rev. B **48**, 7183 (1993).
- ³ M.A. Continentino, *Quantum Scaling in Many Body Systems* (World Scientific, Singapore, 2001).
- ⁴ S. Sachdev, *Quantum Phase Transitions* (Cambridge University Press, Cambridge, 1999).
- ⁵ M. Plischke, and B. Bergersen, *Equilibrium Statistical Physics* (World Scientific, Singapore, 1994).
- ⁶ S.L. Sondhi, S.M. Girvin, J.P. Carini, and D. Shahar, Rev. Mod. Phys. **69**, 315 (1997).
- ⁷ S. Raymond, L.P. Regnault, S. Kambe, J.M. Mignot, P. Lejay, and J. Flouquet, J. Low Temp. Phys. **109**, 205 (1997).
- ⁸ H. Kadowaki, B. Fåk, T. Fukuhara, K. Maezawa, K. Nakajima, M. A. Adams, S. Raymond, and J. Flouquet, Phys. Rev. B **68**, 140402 (2003).
- ⁹ O. Stockert, H. v. Löhneysen, A. Rosch, N. Pyka, and M. Loewenhaupt, Phys. Rev. Lett. **80**, 5627 (1998).
- ¹⁰ G.R. Stewart, Rev. Mod. Phys. **73**, 797 (2001).
- ¹¹ A. Schröder, G. Aeppli, R. Coldea, M.A. Adams, O. Stockert, H. v. Löhneysen, E. Bucher, R. Ramazashvili, and P. Coleman, Nature **407**, 351 (2000).
- ¹² M.C. Aronson, R. Osborn, R.A. Robinson, J.W. Lynn, R. Chau, C.L. Seaman, and M.B. Maple, Phys. Rev. Lett. **75**, 725 (1995).
- ¹³ J.G. Park, D.T. Adroja, K.A. McEwen, and A.P. Murani, J. Phys.: Condens. Matter **14**, 3865 (2002).
- ¹⁴ W. Montfrooij, M.C. Aronson, B.D. Rainford, J.A. Mydosh, A.P. Murani, P. Haen, and T. Fukuhara, Phys. Rev. Lett. **91**, 087202 (2003).
- ¹⁵ W. Bao, Y. Chen, Y. Qiu, and J.L. Sarrao, Phys. Rev. Lett. **91**, 127005 (2003).
- ¹⁶ P. Coleman, and C. Pépin, Physica B **312-313**, 383 (2002).
- ¹⁷ Q. Si, S. Rabello, K. Ingersent, and J.L. Smith, Nature **413**, 804 (2001).
- ¹⁸ T. Moriya, and T. Takimoto, J. Phys. Soc. Japan **64**, 960 (1995).
- ¹⁹ M. Lavagna, and C. Pépin, Phys. Rev. B **62**, 6450 (2000).
- ²⁰ R.A. Fisher, C. Marcenat, N.E. Philips, P. Haen, F. Lapierre, P. Lejay, J. Flouquet, and J. Voiron, J. Low Temp. Phys. **84**, 49 (1991).
- ²¹ S. Kambe, S. Raymond, L.P. Regnault, J. Flouquet, P. Lejay, and P. Haen, J. Phys. Soc. Japan **65**, 3294 (1996).
- ²² L.P. Regnault, W.A.C. Erkelens, J. Rossat-Mignot, P. Lejay, and J. Flouquet, Phys. Rev. B **38**, 4481 (1988).
- ²³ S. Raymond, L.P. Regnault, J. Flouquet, A. Wildes, and P. Lejay, J. Phys.: Condens. Matter **13**, 8303 (2001).
- ²⁴ S. Raymond, W. Knafo, L.P. Regnault, J. Flouquet, A. Wildes, and P. Lejay, Physica B **312-313**, 431 (2002).
- ²⁵ A. Amato, R. Feyherherm, F.N. Gyax, A. Schenck, J. Flouquet, and P. Lejay, Phys. Rev. B **50**, 619 (1994).
- ²⁶ H. Kadowaki, M. Sato, and S. Kawarazaki, Phys. Rev. Lett. **92**, 097204 (2004).
- ²⁷ D.T. Adroja and B.D. Rainford (unpublished).
- ²⁸ N.E. Bickers, D.L. Cox, and J.W. Wilkins, Phys. Rev. Lett. **54**, 230 (1985).
- ²⁹ Y. Kuroda, Y. Ōno, K. Miura, B. Jin, H. Jichu, D. S. Hirashima, and T. Matsuura, Prog. Theor. Phys. Suppl. **108**, 173 (1992).
- ³⁰ L.C. Lopes, Y. Lassailly, R. Julien, and B. Coqblin, J. Magn. Magn. Mater. **31-34**, 251 (1983).
- ³¹ A. Loidl, G. Knopp, H. Spille, F. Steglich, and A.P. Murani, Physica B **76-77**, 376 (1988).
- ³² P. Lehmann, ph-D thesis, Université Louis Pasteur, Strasbourg, 1987.
- ³³ A. Lacerda, A. deVisser, P. Haen, P. Lejay, and J. Flouquet, Phys. Rev. B **40**, 8759 (1989).
- ³⁴ J.H. Van Vleck, *The Theory of Electric and Magnetic Susceptibilities* (Oxford University Press, New York, 1932).
- ³⁵ S. Raymond, L.P. Regnault, S. Kambe, J. Flouquet, and P. Lejay, J. Phys.: Condens. Matter **10**, 2363 (1998).
- ³⁶ P. Haen, J. Flouquet, F. Lapierre, P. Lejay, and G. Remenyi, J. Low. Temp. Phys. **67**, 391 (1987).
- ³⁷ J. Flouquet, S. Kambe, L.P. Regnault, P. Haen, J.P. Brison, F. Lapierre, and P. Lejay, Physica B **215**, 77 (1995).
- ³⁸ J. Flouquet, P. Haen, S. Raymond, D. Aoki, and G. Knebel, Physica B **319**, 251 (2002).
- ³⁹ Y. Kuramoto, Solid State Commun. **63**, 467 (1987).
- ⁴⁰ Y. Kuramoto, Physica B **156-157**, 789, (1989).
- ⁴¹ L.P. Regnault, J.L. Jacoud, J.M. Mignot, J. Rossat-Mignot, C. Vettier, P. Lejay, and J. Flouquet, Physica B **163**, 606 (1990).
- ⁴² H. Wilhelm, S. Raymond, D. Jaccard, O. Stockert, H. v. Löhneysen, and A. Rosch, J. Phys.: Condens. Matter **13**, L329 (2001).
- ⁴³ G. Aeppli, and C. Broholm, *Handbook on the physics and chemistry of rare earths* (Eds. K.A. Gschneidner, L. Eyring, G.H. Lander, and G.R. Chopin, Amsterdam, 1994), vol.19, p. 123.
- ⁴⁴ A.C. Hewson, *The Kondo Problem to Heavy Fermions* (Cambridge University Press, Cambridge, 1993).
- ⁴⁵ A. Schröder, G. Aeppli, E. Bucher, R. Ramazashvili, and P. Coleman, Phys. Rev. Lett. **80**, 5623 (1998).
- ⁴⁶ A. Amato, D. Jaccard, E. Walker, and J. Flouquet, Solid State Commun. **55**, 1131 (1985).
- ⁴⁷ J. Rossat-Mignot, L.P. Regnault, J.L. Jacoud, C. Vettier, P. Lejay, J. Flouquet, E. Walker, D. Jaccard, and A. Amato, J. Magn. Magn. Mater. **38**, 4481 (1988).